

# Zymosan-mediated inflammation impairs in vivo reverse cholesterol transport<sup>S</sup>

Priya Malik,<sup>\*,†</sup> Stela Z. Berisha,<sup>†</sup> Jennifer Santore,<sup>†</sup> Colin Agatista-Boyle,<sup>†</sup> Gregory Brubaker,<sup>†</sup> and Jonathan D. Smith<sup>1,†,§,\*,\*\*</sup>

Department of Molecular Medicine,<sup>\*\*</sup> Cleveland Clinic Lerner College of Medicine of Case Western Reserve University,<sup>\*</sup> Cleveland, OH 44195; and Department of Cell Biology,<sup>†</sup> and Department of Cardiovascular Medicine,<sup>§</sup> Cleveland Clinic, Cleveland, OH 44195

**Abstract** Inflammation has been proposed to impair HDL function and reverse cholesterol transport (RCT). We investigated the effects of inflammation mediated by zymosan, a yeast glucan, on multiple steps along the RCT pathway in vivo and ex vivo. Acute inflammation with 70 mg/kg zymosan impaired RCT to plasma, liver, and feces similarly by 17–22% ( $P < 0.05$ ), with no additional block at the liver. Hepatic gene expression further demonstrated no change in ABCG5, ABCB4, and ABCB11 expression but a decline in ABCG8 mRNA (32%  $P < 0.05$ ). Plasma from zymosan-treated mice had a 21% decrease in cholesterol acceptor ability ( $P < 0.01$ ) and a 35% decrease in ABCA1-specific efflux capacity ( $P < 0.01$ ) in vitro. Zymosan treatment also decreased HDL levels and led to HDL remodeling with increased incorporation of serum amyloid A. In addition, cholesterol efflux from cultured macrophages declined with zymosan treatment in a dose dependant manner. Taken together, our results suggest that zymosan impairs in vivo RCT primarily by decreasing macrophage-derived cholesterol entering the plasma, with minimal additional blocks downstream. Our study supports the notion that RCT impairment is one of the mechanisms for the increased atherosclerotic burden observed in inflammatory conditions.—Malik, P., S. Z. Berisha, J. Santore, C. Agatista-Boyle, G. Brubaker, and J. D. Smith. Zymosan-mediated inflammation impairs in vivo reverse cholesterol transport. *J. Lipid Res.* 2011. 52: 951–957.

**Supplementary key words** high density lipoprotein • cholesterol efflux • macrophages

HDL was first shown to be atheroprotective in the 1970s when the Framingham study found low HDL cholesterol to be the strongest lipoprotein predictor of cardiovascular disease (1). One pathway hypothesized to account for the observed protection is reverse cholesterol transport (RCT)

or the movement of cholesterol from peripheral cells, including lipid laden macrophages, to the liver for excretion. This pathway involves multiple steps including: 1) the efflux of cholesterol to lipid poor apolipoproteins and HDL; 2) the maturation of HDL through cholesterol esterification via lecithin cholesterol acyl transferase; 3) the uptake of HDL cholesterol by the liver; and 4) hepatic cholesterol excretion into the biliary system and feces in the form of bile acids and free cholesterol (2, 3). Thus, understanding the mechanism of RCT and the pathophysiological factors affecting RCT has been a topic of immense research focus with potential clinical significance.

Inflammation may be a potent source of HDL and RCT dysfunction. HDL undergoes multiple structural changes with inflammation rendering it into “acute phase HDL”, which is relatively enriched in free fatty acids, triglycerides, serum amyloid A (SAA), and apolipoprotein (apo)A-IV, whereas cholesterol esters and anti-inflammatory enzymes including paraoxanase 1 are decreased (4–6). In addition, inflammation induces secretion of myeloperoxidase (MPO), which has been shown to modify apoAI and impair its ability to accept cholesterol (7–10). Finally inflammation affects gene expression in the liver, which has consequences for cholesterol uptake and excretion (4, 11, 12). Understanding the mechanisms behind the inflammatory impairment of RCT is clinically relevant as chronic inflammatory conditions such as diabetes, metabolic syndrome, and rheumatoid arthritis are prevalent in our society and associated with an increased atherosclerotic burden (13, 14).

Although a majority of the studies on inflammatory impairment of RCT have been in vitro, two recent studies

*This work was supported by the National Institutes of Health grants HL-066082 and HL-098055 to J.D.S. Its contents are solely the responsibility of the authors and do not necessarily represent the official views of the National Institutes of Health. P.M. was a Howard Hughes Medical Institute Medical Research Training Fellow.*

*Manuscript received 8 September 2010 and in revised form 15 February 2011.*

*Published, JLR Papers in Press, February 19, 2011  
DOI 10.1194/jlr.M011122*

Abbreviations: apo, apolipoprotein; FPLC, fast performance liquid chromatography; LPS, lipopolysaccharide; MPO, myeloperoxidase; RCT, reverse cholesterol transport; SAA, serum amyloid A.

<sup>1</sup>To whom correspondence should be addressed.

e-mail: smithj4@ccf.org

<sup>S</sup>The online version of this article (available at <http://www.jlr.org>) contains supplementary data in the form of two tables and seven figures.

examined the impact of lipopolysaccharide (LPS) on RCT *in vivo* (15, 16). Both showed that LPS inhibits RCT, with the block occurring primarily in cholesterol movement from the liver to the bile. Here, we studied RCT impairment in response to a different inflammatory stimulus: zymosan, a yeast cell wall derived preparation that consists primarily of glucans, mannans, and mannoproteins. Zymosan has been used as an inflammatory stimulus for over 50 years and is especially effective in eliciting MPO release (17, 18). It stimulates the immune system via activation of Toll-like receptor (TLR)2 and dectin 1 whereas LPS acts primarily via TLR4 (19). Using a modified RCT method described by Wang et al. (20), we show that zymosan-mediated inflammation also impairs RCT, but in our model the impairment is primarily due to decreased macrophage-derived cholesterol entering the plasma with minimal additional impact on cholesterol flux through the liver.

## MATERIALS AND METHODS

### Mice

C57BL/6 male mice were purchased from the Jackson Laboratory (Bar Harbor, Maine). Blood was collected either via the tail vein (for initial time points) or via the retro-orbital plexus for the final time point after mice were anesthetized with ketamine/xylazine (170 mg/kg, 5 mg/kg). All experiments were performed in accordance with protocols approved by the Cleveland Clinic Institutional Animal Care and Use Committee.

### In vivo RCT measurement

Mouse bone marrow cells were cultured in DMEM supplemented with 20% L-cell conditioned medium (a source of macrophage-colony stimulating factor) for 12–14 days to generate macrophages. Mature macrophages were subsequently incubated in media containing 2  $\mu\text{Ci/ml}$  [ $^3\text{H}$ ]cholesterol (Amersham) and 50  $\mu\text{g/ml}$  acetylated LDL for 48–72 h to allow foam cell formation. Loaded macrophages were then washed twice and resuspended in DMEM before injection. On average, the cell suspension injected into the mice contained  $\sim 5 \times 10^6$  cells/ml with  $1.2 \times 10^7$  dpm/ml in a 0.25 ml volume.

Mice were housed separately in cages without bedding prior to injection. The [ $^3\text{H}$ ]cholesterol-loaded macrophages were injected subcutaneously (s.c.) into the back flank of mice. Zymosan (Sigma, St. Louis MO) was suspended in sterile PBS to a final concentration of 5 mg/ml and injected intraperitoneally (i.p.) at a final dose of 70 mg/kg ( $\sim 400\mu\text{l}$ ). Control animals received i.p. injections of PBS. To quantify the injected radioactivity, an aliquot of the cells was spun down, cholesterol extracted in hexane:isopropanol (3:2), and radioactivity determined via liquid scintillation counting.

Blood was collected at 24 h intervals for 3 or 4 days (as specified in the text and figure legends), plasma radioactivity was measured, and total plasma dpm was calculated by estimating plasma volume as 3.85% of the body weight. RCT to the plasma compartment was calculated as  $100 \times \text{total plasma dpm}/\text{injected cell dpm}$ . Feces were collected daily, hydrated in a 50% ethanol solution, homogenized, and spiked with 10,000 dpm of [ $^{14}\text{C}$ ]cholesterol (Amersham) as an internal recovery standard. Radioactivity in a 0.3 ml aliquot of the fecal homogenate was then quantified via liquid scintillation counting after keeping feces in the dark for 24 h to reduce chemiluminescence, and the [ $^{14}\text{C}$ ]cholesterol dpm was used to calculate the [ $^3\text{H}$ ]cholesterol in the entire fecal

homogenate. RCT to the fecal compartment was calculated as the percent of the injected cell dpm. Liver RCT was quantified in a similar manner as the fecal RCT. Thus, RCT is represented as the percentage of injected cholesterol counts appearing in the plasma, liver, or fecal compartments.

### Ex vivo macrophage cholesterol efflux studies

RAW 264.7 murine macrophages in 24-well plates were labeled by incubation in media containing 1  $\mu\text{Ci/ml}$  [ $^3\text{H}$ ]cholesterol for 24 h. ABCA1 activity was induced with 0.3 mM 8Br-cAMP (Sigma, St. Louis MO) in some of the wells as previously described (21). The cells were washed and chased for 4 h in serum-free medium in the presence of 0.4% plasma and 8Br-cAMP (for the pretreated wells). Radioactivity in the media was counted directly, whereas radioactivity in the cells was determined after extraction with hexane:isopropanol (3:2). The percent cholesterol efflux was calculated as  $100 \times (\text{medium dpm})/(\text{medium dpm} + \text{cell dpm})$ . The ABCA1 specific efflux was calculated as the difference between efflux in the presence of 8Br-cAMP (total efflux) and the absence of 8Br-cAMP (ABCA1 independent efflux). When used, zymosan was present in the media 4 h prior to and during the chase. In some efflux experiments, bone marrow macrophages were substituted for RAW264.7 cells after being cultured in conditions described above.

### Plasma cholesterol and protein analyses

Plasma was collected from mice 72 h after treatment with either saline or zymosan and total cholesterol and HDL cholesterol levels were quantified enzymatically (StanBio, Houston, TX). Mouse SAA levels were quantified by ELISA (Invitrogen, Carlsbad, CA). Fast performance liquid chromatography (FPLC) was performed on pooled plasma from 3–4 mice on a Superose 6 column (Amersham, Uppsala, Sweden) with 0.5ml fractions collected. Total cholesterol levels in the FPLC fractions were measured enzymatically via the Amplex Red cholesterol assay (Invitrogen). Aliquots of the FPLC fractions were then reduced using DTT, separated by SDS-PAGE, transferred to nitrocellulose membranes, and probed with primary antibodies to mouse apoA1 (Bioscience Resource Project, Sacramento, CA), apoE (Santa Cruz Biotech, Santa Cruz, CA), and apoB48 (gift from Dr. Stephen Young, UCLA). Blots were visualized via chemiluminescence (ECL plus kit, GE Healthcare).

### Preparation of RNA and gene expression analysis

Livers of control and zymosan-treated mice were recovered 48 h after treatment, homogenized in Trizol reagent (Invitrogen), and RNA was purified using the RNeasy Fibrous Mini Kit (Qiagen, Valencia, CA) with on-column DNase digestion. Total RNA was then used to probe MouseRef-8 V2 chips (Illumina Inc., San Diego, CA). The data was processed by quantile normalization using Illumina BeadStudio software. Bone marrow macrophage RNA was prepared using the RNeasy Mini Kit (Qiagen). Liver and bone marrow macrophage RNA was subjected to quantitative real-time PCR analysis. Total RNA (1.5  $\mu\text{g}$ ) was used to synthesize first-strand cDNA with random primers, using the SuperScript VILO cDNA synthesis kit (Invitrogen). cDNA was purified by using QIAquick PCR Purification kit (Qiagen) and used as a template in quantitative real-time-PCR reactions. TaqMan qRT-PCR assays (Applied Biosystems, Foster City, CA) were used to quantify the mRNA levels of ApoA1, ApoE, Abca1, Abcg1, Ldlr, and Scarb1. The expression of these transcripts was measured relative to the ubiquitin C (Ubc) endogenous control transcript using the  $\Delta\Delta\text{C}_T$  method.

### Statistical analysis

Data are reported as mean  $\pm$  SD. Unpaired two-tailed *t*-tests were used to determine the difference between control and

zymosan-treated mice. Comparisons of three or more groups were performed by ANOVA with Newman-Keuls posttest. Statistics were performed using Prism 4 software (GraphPad Software Inc., San Diego, CA). Microarray expression data was subjected to permutation analysis to determine the false discovery rate using the Significance Analysis of Microarray plugin for Microsoft Excel (22).

## RESULTS

### Zymosan-mediated inflammation impedes *in vivo* RCT

To examine the effect of zymosan-mediated inflammation on RCT, we followed movement of [<sup>3</sup>H]cholesterol from injected macrophages to the plasma, liver, and fecal compartments. The 70 mg/kg dose of zymosan was selected through pilot studies, which revealed a robust effect on mice at 24 h, causing an 8% loss of body weight and 40% decrease in fecal mass. However, these effects were transient; body weight recovered to match the control mice by 48 h, and the cumulative fecal mass was the same as in control mice by 72 h. Over a 4 day period following a single zymosan injection, RCT to the plasma and fecal compartments was consistently decreased compared with the saline-treated animals (Fig. 1A, B). Pooled data from five independent studies demonstrated that zymosan treatment resulted in RCT that was 17% lower in the plasma ( $P < 0.001$ ), 22% lower in the liver ( $P < 0.05$ ), and 20% lower in the feces ( $P < 0.001$ ) at the 72 h time point (Fig. 1C). Because RCT is similarly impaired in each successive compartment (plasma, liver, feces) by 17–22%, this indicates that the primary RCT block in our inflammation model is at the entry of macrophage-derived [<sup>3</sup>H]cholesterol into the plasma.

### Effects of zymosan-mediated inflammation on hepatic gene expression

As previous studies have shown downregulation of hepatic cholesterol transporters with LPS-induced inflammation concurrent with a decrease in fecal RCT (15, 16), we examined the global effects of zymosan, using microarrays, on hepatic gene expression 48 h after treatment ( $N = 4$  each condition). Out of the 25,967 probes on the chip, 11,235 were expressed above background ( $P < 0.05$ ) in at least four of the eight samples and further analyzed. Of these 11,235 probes, 11.4% (1287 probes) were differentially expressed ( $P < 0.05$ ) in the livers from zymosan-treated mice when compared with controls, with a false discovery rate of 34%. The genes with the highest levels of up- and down-regulation are listed in supplementary Table I. A volcano plot illustrating changes in global hepatic gene expression between zymosan- and saline-treated animals is shown in supplementary Fig. I. Using Ingenuity Pathway Analysis software, the top three canonical pathways associated with the differentially expressed genes were acute phase response signaling, fatty acid metabolism, and hepatic cholestasis. Individual genes with altered expression within these pathways are listed in supplementary Table II.

Focusing on genes involved in lipid metabolism and secretion, we found no significant zymosan-mediated changes in the mRNA levels of the transporters ABCG5,

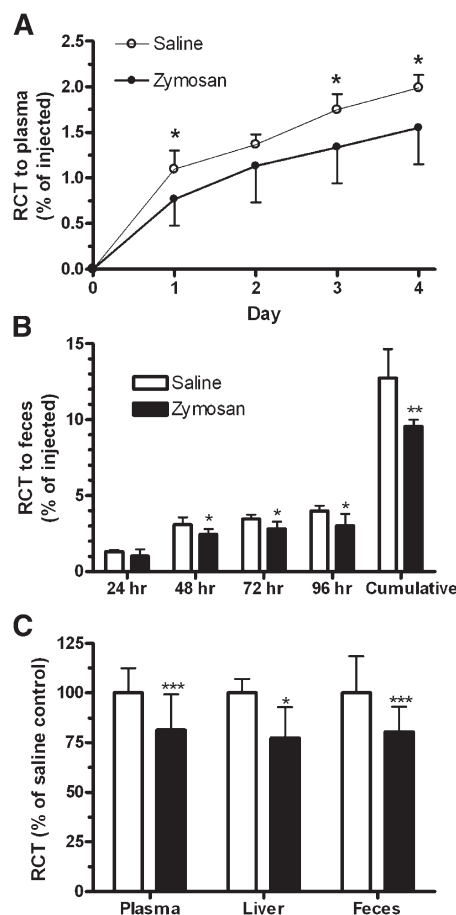


**Fig. 1.** Zymosan impairs RCT *in vivo*. A representative study showing plasma (A) and fecal (B) RCT (% of the injected [<sup>3</sup>H]cholesterol counts) over a 4 day period following 70 mg/kg zymosan injection ( $n = 6$  each treatment). C: RCT 72 h after zymosan treatment to the plasma ( $n = 26$  each), liver ( $n = 5$  each), and fecal ( $n = 26$  each) compartments. Plasma and fecal RCT was measured over five independent studies and all measures were normalized within each study to saline-injected control values. Open symbols and bars represent saline-injected controls; closed symbols and bars represent zymosan treatment. \*  $P < 0.05$ ; \*\*  $P < 0.01$ ; \*\*\*  $P < 0.001$  versus saline control.

ABCB4, or ABCB11 involved in the hepatic secretion of free cholesterol, phospholipid, and bile salts, respectively (Fig. 2A). However, zymosan treatment led to a significant 32% decrease in the expression of ABCG8 ( $P < 0.05$ ), another transporter involved in free cholesterol excretion. CYP27A1 and CYP8B1 mRNAs, encoding enzymes involved in the alternative bile acid synthesis pathway, were also significantly decreased by zymosan treatment ( $P < 0.05$ ). CYP7A1 mRNA also decreased, encoding a key enzyme in the canonical bile acid synthesis pathway, but this decrease failed to reach statistical significance (Fig. 2B). Hepatic apoA1 mRNA levels were unchanged by the zymosan treatment ( $0.94 \pm 0.08$ -fold vs. control,  $P = 0.17$ ), which we confirmed by quantitative real-time-PCR ( $1.21 \pm 0.41$ -fold vs. control,  $P = 0.41$ ). Hepatic scavenger receptor-BI (SR-BI, encoded by the Scarb1 gene) expression on the Illumina expression array was not detectable above background, which we attribute to poor probe design. Thus, we measured

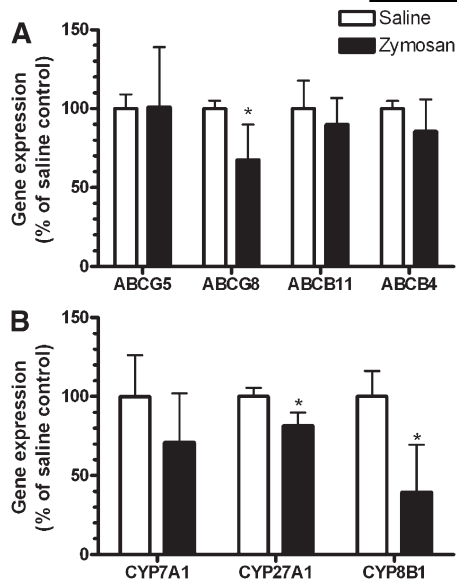


**Fig. 2.** Zymosan effects on expression of selected hepatic mRNAs. **A:** Hepatic expression of ABCG5, ABCB11, and ABCB4 mRNAs were unchanged 72 h after zymosan treatment, whereas ABCG8 mRNA levels were decreased by 32%. **B:** Expression of CYP27A1 and CYP8B1 mRNAs were significantly decreased and CYP7A1 mRNA levels were lower but not significantly different after zymosan treatment. N = 4 each treatment; \*  $P < 0.05$  versus saline control.

SR-BI mRNA by quantitative real-time-PCR and found that its levels were not altered by zymosan treatment (1.17 ± 0.29-fold,  $P = 0.46$ ).

#### Effects of zymosan-mediated inflammation on plasma lipoproteins

Plasma HDL levels were decreased by 19% ( $P < 0.01$ , n = 9 saline and n = 10 zymosan) 72 h after induction of inflammation but the changes in total cholesterol levels were only of borderline significance ( $P = 0.06$ , Fig. 3A). FPLC of pooled plasma samples confirmed less cholesterol in the apoA1 containing HDL fractions (#22–26) after zymosan treatment (Fig. 3B, D). Zymosan treatment did not alter the size of the apoA1-containing HDL particles on the FPLC profile (Fig. 3B), which was confirmed by nondenaturing gradient gel electrophoresis (supplementary Fig. II). As has been previously reported for LPS (15), zymosan inflammation resulted in increased cholesterol in the apoB containing LDL fractions (#14–18) (Fig. 3B, D). In addition, Western blot analysis showed that zymosan treatment led to an increased distribution of apoE particles in fractions 12–26 spanning the IDL, LDL, and HDL regions (Fig. 3D). Overall plasma levels of apoE increased nearly 2-fold with zymosan-mediated inflammation (supplementary Fig. III) as has been reported previously in other mouse inflammation models (23), despite a trend toward lower apoE hepatic mRNA expression in the microarray study (0.93 ± 0.08-fold vs. control,  $P = 0.11$ ).

As expected, there was a marked induction of SAA with zymosan treatment, leading to a 7-fold increase in hepatic SAA mRNA expression (supplementary Table I,  $P < 0.001$ ) and 13-fold increase in plasma SAA protein levels (Fig. 3C,

$P < 0.001$ ). A separate study was performed showing that zymosan led to large increases in plasma SAA levels on days 1, 2, and 3 after the zymosan challenge (supplementary Fig. IV). Analysis of the FPLC samples revealed SAA to be completely localized to the apoA1-containing HDL fractions (#22–26) (Fig. 3D), suggesting that HDL was remodeled with SAA incorporation. Plasma apoA1 levels were analyzed by Western blot from nine saline controls and 11 zymosan-treated mice over two separate experiments. Densitometry from the two experiments pooled revealed only a nonsignificant 3% decrease in plasma apoA1 in the zymosan-treated mice ( $P = 0.68$ , supplementary Fig. V B).

#### Zymosan-mediated inflammation impairs plasma efflux capacity and macrophage efflux function in vitro

To further examine the mechanism for the block in RCT to the plasma compartment, we tested the ability of plasma from zymosan-treated mice to promote ABCA1-dependent and -independent efflux from cholesterol-loaded RAW264.7 macrophages. First, we performed a plasma dose response curve to determine the concentration at which efflux to plasma is saturated. We observed that cholesterol efflux increased linearly with plasma concentration up to a concentration of 0.5% in the media (supplementary Fig. VI). At higher plasma concentrations, there appeared to be saturation of the macrophage machinery that mediates efflux. We therefore used a 0.4% concentration of plasma for all subsequent experiments. Plasma from zymosan-treated mice had 21% less cholesterol acceptor activity than controls ( $P < 0.01$ , Fig. 4A). This difference was accounted for by a 35% ( $P < 0.01$ ) reduction in ABCA1-dependent activity (Fig. 4A) without any change in the ABCA1-independent acceptor activity. This suggests that part of the block in RCT with zymosan treatment is due to fewer functionally competent ABCA1-dependent cholesterol acceptors in the plasma of zymosan-treated mice.

We next examined the impact of zymosan treatment of macrophages ex vivo. Zymosan pretreatment inhibited cholesterol efflux from bone marrow macrophages to untreated plasma in a dose-dependent manner with 22% inhibition at 60 µg/ml ( $P < 0.01$ , Fig. 4B), a dose that we estimate is similar to the concentration achieved in our in vivo studies. We obtained similar results by zymosan pretreatment of cholesterol labeled and loaded RAW264.7 cells, where we determined that this inhibition was accounted for by a reduction in ABCA1-specific efflux (Fig. 4C). We further examined ex vivo zymosan-mediated changes in the expression of selected genes in bone marrow derived macrophages (supplementary Fig. VII). We observed moderate but significant decreases in Scarb1 (31% decreased) and Ldlr (32% decreased) mRNAs in response to zymosan, whereas ApoE mRNA decreased by 54%. Examining the cholesterol efflux transporters, we observed a significant induction of Abca1 mRNA by 56%, whereas Abcg1 mRNA was not significantly altered. Thus, the reduced ABCA1 efflux activity in zymosan-treated macrophages cannot be accounted for by effects on ABCA1

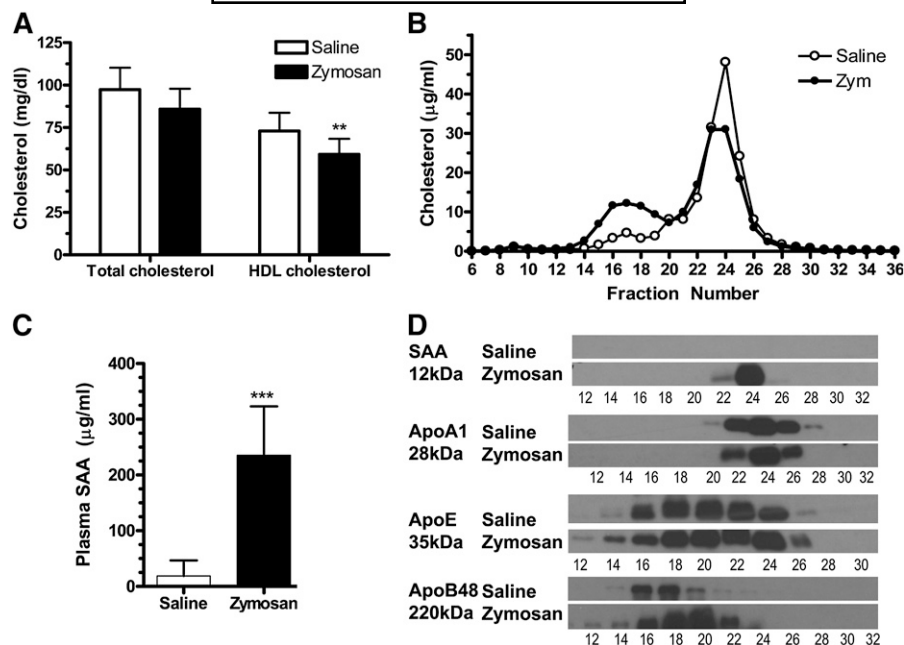


**Fig. 3.** Zymosan effects on plasma lipoproteins (72 h time point). **A:** Plasma total cholesterol levels were not significantly altered whereas HDL-cholesterol decreased by 19% after zymosan treatment ( $n = 10$ ) versus controls ( $n = 9$ ;  $** P < 0.01$ ). **B:** FPLC cholesterol profile of pooled plasma samples from zymosan- and saline-treated mice ( $n = 4$  in each pool). **C:** Plasma SAA levels measured by ELISA increased >13-fold after zymosan treatment ( $n = 10$  each;  $*** P < 0.001$ ). **D:** Western blot analysis of SAA, apoA1, apoE, and apoB48 in even-numbered FPLC fractions.

mRNA. In addition, the zymosan-mediated increases in plasma apoE cannot be accounted for by increased macrophage apoE mRNA.

## DISCUSSION

The atheroprotective pathway of RCT is a multistep process that requires the synergistic action of multiple players, many of which are impaired with inflammation. Here we show that in vivo exposure to zymosan led to decreased HDL-cholesterol, decreased plasma cholesterol acceptor activity, and changes in hepatic gene expression. In addition, we found that ex vivo exposure of macrophages to zymosan decreased cholesterol efflux. The end result of zymosan treatment in mice was an overall decrease in macrophage-derived cholesterol appearing in the plasma, liver, and feces. While our experiments were in progress, two additional studies were published that confirmed the basic finding of reduced RCT with inflammation, but in response to different stimulus: the bacterial endotoxin LPS (15, 16). Using zymosan as an alternate model of inflammation, our results have several differences from these published reports, including the primary site at which RCT was impaired.

In our study, zymosan impaired RCT to the plasma, liver, and feces by a similar magnitude (17–22%), indicating that the primary block occurred at the level of macrophage-derived cholesterol entering the plasma without an additional block at the liver. In contrast, McGillicuddy et al. (15) and Annema et al. (16) demonstrated that the liver acted as a gatekeeper in inhibiting excretion of

cholesterol into bile upon inflammation with LPS. Both studies showed a marked 70–80% inhibition of bile and fecal RCT and a small transient 20–30% decline in plasma RCT with no changes in RCT to the liver upon LPS treatment (12, 15). These differences are most likely due to the use of different inflammatory stimuli and the severity of their effects on the liver and intestine. Zymosan is recognized by dectin-1, TLR2, and CD14 receptors, whereas the effects of *Escherichia coli*-derived LPS are primarily mediated by TLR4 (19). This difference in receptors can lead to altered impact on gene expression and lipoprotein metabolism. LPS has been shown in multiple studies to drastically affect liver cholesterol transporters with up to a 90% decline in ABCG5, ABCG8, and CYP7A1 mRNA and protein levels (12, 15). However, in our microarray data, ABCG5 mRNA levels were unaffected by zymosan. Although ABCG8 and CYP7A1 mRNA levels were lower after zymosan, the downregulation was not as drastic as has been reported with LPS treatment. Thus, the absence of drastic changes in liver gene expression with altered activation of the innate immune system in our zymosan-mediated inflammation model may explain why the hepatic cholesterol excretion pathway remained largely intact.

We also examined the inflammatory impairment of RCT for a longer time course, up to four days after the inflammatory insult when the metabolic effects of the acute inflammatory reaction had subsided, whereas McGillicuddy et al. and Annema et al. studied the inflammatory RCT impairment for only two days. The longer time course is significant as acute inflammation with zymosan induced a catabolic state in mice with lower food consumption, a

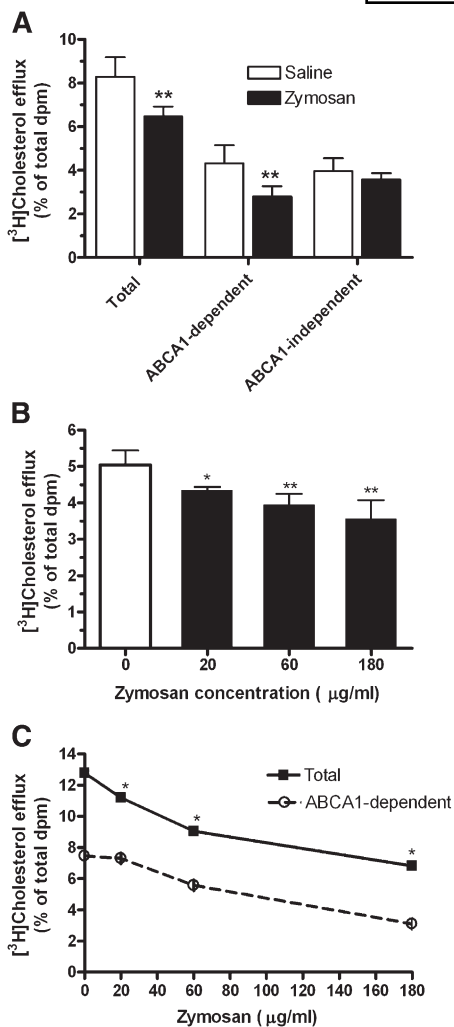


**Fig. 4.** Zymosan treatment impairs plasma efflux capacity and macrophage efflux function. **A:** Plasma from saline- and zymosan-treated mice ( $n = 5$  each) was obtained 72 h after treatment and used at 0.4% concentration as an efflux acceptor from cholesterol labeled and loaded RAW264.7 cells. Total and ABCA1-dependent efflux were significantly reduced after zymosan treatment (\*\* $P < 0.01$ ), whereas ABCA1-independent efflux was unchanged. **B:** Pretreatment of cholesterol loaded and labeled bone marrow macrophages with zymosan led to a dose-dependent inhibition of cholesterol efflux to 0.4% control plasma acceptor ( $n = 3-6$  wells for each zymosan dose; \* $P < 0.05$ ; \*\* $P < 0.01$  vs. 0 dose by ANOVA posttest). **C:** Pretreatment of cholesterol loaded RAW264.7 cells with zymosan led to a dose-dependent inhibition of cholesterol efflux to a 0.4% control plasma acceptor ( $n = 2$ , each zymosan dose). Total and ABCA1-independent activity were determined in the presence and absence of 0.3 mM 8Br-cAMP and the difference was used to determine ABCA1-dependent efflux. (\* $P < 0.05$  vs. 0 dose by ANOVA posttest).

5–7% drop in body weight, and a 40% decline in fecal mass in the first 24 h. However, body weight and cumulative fecal output were comparable to the saline-treated control mice at the 48 and 72 h time points, respectively. LPS treatment may lead to more pronounced metabolic effects, as Annema et al. (16) observed a 34% decline in fecal production over their 48 h study, whereas McGillicuddy et al. (15) did not specify the changes in fecal production. Lower caloric intake and decreased fecal mass


could impact fecal RCT by a nonspecific mechanism; by increasing the time course of our experiments, we sought to minimize the confounding effects of lower fecal mass on fecal RCT. Therefore, some of the differences in our results may be due to the milder effects of zymosan on the liver and intestines, the more rapid recovery of appetite and fecal production, and our examination of RCT after the original inflammatory response had subsided.

Finally, we also used a modified RCT protocol in which [ $^3\text{H}$ ]cholesterol-labeled macrophages were injected s.c. and the inflammatory stimulus injected i.p., whereas both were injected i.p. in the study performed by Annema et al. (16). This modification of the RCT protocol with the macrophages injected s.c. rather than i.p. has been previously described by Wang et al. (20) who showed that both injection sites yield similar RCT values. However, s.c. versus i.p. foam cell injection conferred the benefits of decreased variability and increased reproducibility due to lower number of injections hitting the intestines of landing too superficially (20). However, it is unclear what effect, if any, this modification has on the differences in our experimental results.

Because the primary block in RCT with zymosan-mediated inflammation appeared to be due to decreased macrophage-derived cholesterol entering the plasma, we further investigated the mechanisms responsible for this block. Our in vitro studies showed that plasma from zymosan-treated mice had 21% decreased cholesterol acceptor activity that was accounted for by a 35% decrease in ABCA1-dependent acceptor activity. This may be partially due to the significant 18% decrease in HDL-cholesterol levels, although plasma apoA1 levels were not significantly changed after zymosan treatment. In addition, inflammation is known to affect HDL quality. Studies from our group (7) as well as Heinecke's group (10) have shown that apoA1 can undergo oxidative modifications, rendering it dysfunctional with decreased cholesterol acceptor activity. Inflammation is known to contribute to oxidative stress, and indeed the level of oxidation in apoA1 isolated from patients with cardiovascular disease was correlated with decreased cholesterol acceptor activity (7). Further, the HDL particle itself undergoes remodeling with inflammation, with enrichment of SAA and secretory phospholipase A2 (4). Lipoprotein analysis in our studies confirmed that zymosan treatment led to a marked induction of SAA and its enrichment in HDL particles. There is some controversy in the published literature regarding how SAA affects HDL function. De Beer and colleagues (6, 24) believe that acute-phase HDL enriched with SAA is a more efficient acceptor of cholesterol (and therefore atheroprotective). However, this is contradicted by other reports that showed decreased cholesterol efflux ability and overall RCT with SAA-enriched acute-phase HDL (16, 25). In our study, plasma from zymosan-treated mice with SAA-enriched HDL had a diminished efflux capacity, but it is unclear what role, if any, SAA plays in this response.

Zymosan also directly inhibited the macrophage's ability to participate in efflux. In our experiments with RAW264.7 cells, this decrease is primarily due to impairment of ABCA1 efflux. Previous in vivo RCT studies have

shown that ABCA1 and ABCG1 are the primary pathways for foam cell cholesterol efflux (26); downregulation of both can occur with LPS or cytokine treatment in multiple macrophage cell lines (12, 15, 27). Furthermore, mouse macrophages treated with LPS or its component lipid A have impaired ABCA1 mediated cholesterol to apoAI (28, 29). These findings suggest that inflammatory impairment of foam cell cholesterol efflux capacity contributes to the reduction in RCT. However, the regulation of ABCA1 activity by zymosan appears to be posttranscriptional and/or posttranslational, as ABCA1 mRNA was actually higher in zymosan-treated cells. Recently, MyD88, a toll-like receptor signal transduction mediating protein was found to promote ABCA1 mRNA levels (30), and we speculate that zymosan's induction of ABCA1 mRNA may be mediated through TLR2 and MyD88.

In conclusion, we present evidence here to support the hypothesis that zymosan-mediated inflammation impairs RCT. The impairment primarily appears to be from decreased macrophage-derived [<sup>3</sup>H]cholesterol entering the plasma, specifically associated with a combination of decreased macrophage efflux function and decreased ability of plasma to accept cholesterol via ABCA1, although the precise mechanisms for these findings have not been elucidated. In contrast to previously published reports, we see no block in RCT at the liver and a thorough analysis of hepatic gene expression demonstrated only small changes in genes involved in hepatic cholesterol metabolism. Our study supports the growing literature that inflammation from multiple sources can cause a multistep RCT impairment and contribute to increased atherosclerosis. 

## REFERENCES

- Gordon, T., W. P. Castelli, M. C. Hjortland, W. B. Kannel, and T. R. Dawber. 1977. High density lipoprotein as a protective factor against coronary heart disease. The Framingham Study. *Am. J. Med.* **62**: 707–714.
- Tall, A. R. 2008. Cholesterol efflux pathways and other potential mechanisms involved in the athero-protective effect of high density lipoproteins. *J. Intern. Med.* **263**: 256–273.
- Rader, D. J., E. T. Alexander, G. L. Weibel, J. Billheimer, and G. H. Rothblat. 2009. The role of reverse cholesterol transport in animals and humans and relationship to atherosclerosis. *J. Lipid Res.* **50**(Suppl): S189–S194.
- Khovidhunkit, W., M. S. Kim, R. A. Memon, J. K. Shigenaga, A. H. Moser, K. R. Feingold, and C. Grunfeld. 2004. Effects of infection and inflammation on lipid and lipoprotein metabolism: mechanisms and consequences to the host. *J. Lipid Res.* **45**: 1169–1196.
- Kontush, A., and M. J. Chapman. 2006. Functionally defective high-density lipoprotein: a new therapeutic target at the crossroads of dyslipidemia, inflammation, and atherosclerosis. *Pharmacol. Rev.* **58**: 342–374.
- van der Westhuyzen, D. R., F. C. de Beer, and N. R. Webb. 2007. HDL cholesterol transport during inflammation. *Curr. Opin. Lipidol.* **18**: 147–151.
- Zheng, L., B. Nukuna, M. L. Brennan, M. Sun, M. Goormastic, M. Settle, D. Schmitt, X. Fu, L. Thomson, P. L. Fox, et al. 2004. Apolipoprotein A-I is a selective target for myeloperoxidase-catalyzed oxidation and functional impairment in subjects with cardiovascular disease. *J. Clin. Invest.* **114**: 529–541.
- Zheng, L., M. Settle, G. Brubaker, D. Schmitt, S. L. Hazen, J. D. Smith, and M. Kinter. 2005. Localization of nitration and chlorination sites on apolipoprotein A-I catalyzed by myeloperoxidase in human atheroma and associated oxidative impairment in ABCA1-dependent cholesterol efflux from macrophages. *J. Biol. Chem.* **280**: 38–47.
- Bergt, C., G. Marsche, U. Panzenboeck, J. W. Heinecke, E. Malle, and W. Sattler. 2001. Human neutrophils employ the myeloperoxidase/hydrogen peroxide/chloride system to oxidatively damage apolipoprotein A-I. *Eur. J. Biochem.* **268**: 3523–3531.
- Bergt, C., S. Pennathur, X. Fu, J. Byun, K. O'Brien, T. O. McDonald, P. Singh, G. M. Anantharamaiah, A. Chait, J. Brunzell, et al. 2004. The myeloperoxidase product hypochlorous acid oxidizes HDL in the human artery wall and impairs ABCA1-dependent cholesterol transport. *Proc. Natl. Acad. Sci. USA.* **101**: 13032–13037.
- Memon, R. A., A. H. Moser, J. K. Shigenaga, C. Grunfeld, and K. R. Feingold. 2001. In vivo and in vitro regulation of sterol 27-hydroxylase in the liver during the acute phase response. potential role of hepatocyte nuclear factor-1. *J. Biol. Chem.* **276**: 30118–30126.
- Khovidhunkit, W., A. H. Moser, J. K. Shigenaga, C. Grunfeld, and K. R. Feingold. 2003. Endotoxin down-regulates ABCG5 and ABCG8 in mouse liver and ABCA1 and ABCG1 in J774 murine macrophages: differential role of LXR. *J. Lipid Res.* **44**: 1728–1736.
- Hansson, G. K. 2005. Inflammation, atherosclerosis, and coronary artery disease. *N. Engl. J. Med.* **352**: 1685–1695.
- Kaplan, M. J. 2009. Management of cardiovascular disease risk in chronic inflammatory disorders. *Nat. Rev. Rheumatol.* **5**: 208–217.
- McGillicuddy, F. C., M. de la Llera Moya, C. C. Hinkle, M. R. Joshi, E. H. Chiquoine, J. T. Billheimer, G. H. Rothblat, and M. P. Reilly. 2009. Inflammation impairs reverse cholesterol transport in vivo. *Circulation.* **119**: 1135–1145.
- Annema, W., N. Nijstad, M. Tolle, J. F. de Boer, R. V. Buijs, P. Heeringa, M. van der Giet, and U. J. Tietge. 2010. Myeloperoxidase and serum amyloid A contribute to impaired in vivo reverse cholesterol transport during the acute phase response but not group IIA secretory phospholipase A2. *J. Lipid Res.* **51**: 743–754.
- Zhang, R., M. L. Brennan, Z. Shen, J. C. MacPherson, D. Schmitt, C. E. Molenda, and S. L. Hazen. 2002. Myeloperoxidase functions as a major enzymatic catalyst for initiation of lipid peroxidation at sites of inflammation. *J. Biol. Chem.* **277**: 46116–46122.
- Di Carlo, F. J., and J. V. Fiore. 1958. On the composition of zymosan. *Science.* **127**: 756–757.
- Gantner, B. N., R. M. Simmons, S. J. Canavera, S. Akira, and D. M. Underhill. 2003. Collaborative induction of inflammatory responses by dectin-1 and Toll-like receptor 2. *J. Exp. Med.* **197**: 1107–1117.
- Wang, M. D., V. Franklin, and Y. L. Marcel. 2007. In vivo reverse cholesterol transport from macrophages lacking ABCA1 expression is impaired. *Arterioscler. Thromb. Vasc. Biol.* **27**: 1837–1842.
- Smith, J. D., M. Miyata, M. Ginsberg, C. Grigaux, E. Shmookler, and A. S. Plump. 1996. Cyclic AMP induces apolipoprotein E binding activity and promotes cholesterol efflux from a macrophage cell line to apolipoprotein acceptors. *J. Biol. Chem.* **271**: 30647–30655.
- Tusher, V. G., R. Tibshirani, and G. Chu. 2001. Significance analysis of microarrays applied to the ionizing radiation response. *Proc. Natl. Acad. Sci. USA.* **98**: 5116–5121.
- Li, L., P. A. Thompson, and R. L. Kitchens. 2008. Infection induces a positive acute phase apolipoprotein E response from a negative acute phase gene: role of hepatic LDL receptors. *J. Lipid Res.* **49**: 1782–1793.
- van der Westhuyzen, D. R., L. Cai, M. C. de Beer, and F. C. de Beer. 2005. Serum amyloid A promotes cholesterol efflux mediated by scavenger receptor B-I. *J. Biol. Chem.* **280**: 35890–35895.
- Artl, A., G. Marsche, S. Lestavel, W. Sattler, and E. Malle. 2000. Role of serum amyloid A during metabolism of acute-phase HDL by macrophages. *Arterioscler. Thromb. Vasc. Biol.* **20**: 763–772.
- Wang, X., H. L. Collins, M. Ranalletta, I. V. Fuki, J. T. Billheimer, G. H. Rothblat, A. R. Tall, and D. J. Rader. 2007. Macrophage ABCA1 and ABCG1, but not SR-BI, promote macrophage reverse cholesterol transport in vivo. *J. Clin. Invest.* **117**: 2216–2224.
- Baranova, I., T. Vishnyakova, A. Bocharov, Z. Chen, A. T. Remaley, J. Stonik, T. L. Eggerman, and A. P. Patterson. 2002. Lipopolysaccharide down regulates both scavenger receptor B1 and ATP binding cassette transporter A1 in RAW cells. *Infect. Immun.* **70**: 2995–3003.
- Castrillo, A., S. B. Joseph, S. A. Vaidya, M. Haberland, A. M. Fogelman, G. Cheng, and P. Tontonoz. 2003. Crosstalk between LCR and toll-like receptor signaling mediates bacterial and viral antagonism of cholesterol metabolism. *Mol. Cell.* **12**: 805–816.
- Majdalawieh, A., and H-Y. Ro. 2009. LPS-induced suppression of macrophage cholesterol efflux is mediated by adipocyte enhancer-binding protein 1. *Int. J. Biochem. Cell Biol.* **41**: 1518–1525.
- Smook, K. A., J. J. Aloor, J. Madenspacher, B. A. Merrick, J. B. Collins, X. Zhu, G. Cavigliolo, M. N. Oda, J. S. Parks, and M. B. Fessler. 2010. Myeloid differentiation primary response protein 88 couples reverse cholesterol transport to inflammation. *Cell Metab.* **11**: 493–502.